1992 SCA Conference Paper Number 9219

Use of NMR Imaging For Determining Fluid Saturation Distributions During Multiphase Displacement in Porous Media

Kyung-Hoe Kim, Songhua Chen, Fangfang Qin and A. Ted Watson

Department of Chemical Engineering
Texas A&M University
College Station, TX 77843-3122

ABSTRACT

The use of nuclear magnetic resonance imaging for determination of porosity and saturation distributions is demonstrated. Profile images are obtained during displacement experiments, whereby one fluid phase in a porous media is immiscibly displaced by another, as well as under static conditions. Procedures are developed to estimate the intrinsic intensity of magnetization from the measured profile images. The intrinsic intensity of magnetization is then scaled to determine saturation and porosity. The spatial and saturation dependence of transverse relaxation is considered in estimating the intrinsic magnetization, and procedures for selection of appropriate relaxation models are provided. Results obtained for several limestone samples are presented.

INTRODUCTION

Many reservoir processes involve the flow of two immiscible fluid phases (e.g. oil and water) or three phases (e.g., oil, water and gas). The determination of fluid saturation distributions and porosity in porous media is a fundamental measurement to characterize fluid transport and storage in reservoir rocks. Saturation and porosity are also intermediate quantities that are required to estimate most of the basic petrophysical properties concerning the flow of multiple fluid phases in porous media, such as relative permeability and capillary pressure functions.

Magnetic resonance imaging (MRI) provides new opportunities for characterizing fluid distributions in porous media (Baldwin et al., 1986; Chen et al., 1988; Edelstein et al., 1988). In this work we investigate the use of MRI for monitoring fluid saturation distributions during two-phase displacement experiments. Deuterium oxide is used as the aqueous phase, and the oil phase is observed by detection at the proton resonance frequency. Profile images, which represent signal intensity of magnetization as a function of a single spatial dimension, can be acquired very quickly with MRI and are thus suitable for monitoring saturation distributions during dynamic displacement experiments. Longitudinal profile images are most useful for situations in which the sample and fluid distributions are relatively uniform in the transverse direction. Information about the longitudinal saturation distribution in both steady state and dynamic displacement experiments can be used with implicit estimation procedures to substantially improve the accuracy with which relative permeability and capillary pressure functions can be estimated (Richmond and Watson, 1990; Watson et al, 1991).

Considerable effort can be required to accurately determine saturation or porosity from measured profile images. Quantitative characterization is based on the fact that the intrinsic (or equilibrium) intensity of magnetization is proportional to the number of observed protons. However, fluid transverse relaxation in porous media is so fast that significant relaxation can occur during signal acquisition. Previously, Mandava et al (1990) presented a method to estimate saturation and porosity distributions from MRI profile images. The method was based on assumptions that transverse relaxation can be represented as a first-order (single-exponential) process, and that the relaxation process does not depend on saturation or location. Significant errors in property estimates can be encountered when these assumptions are not met (Chen et al., 1991). In this paper, we develop a new approach for obtaining quantitative estimates of porosity and saturation distributions from MRI images in which the effects of spatial variation and saturation dependence of transverse relaxation are taken into account. Also, we investigate the use of different models for representation of transverse relaxation.

THEORY

In the usual development of profile images (Mansfield, 1982; Mandava et al., 1990), the intensity of magnetization at the echo time is determined in the frequency domain. The following equation provides a relationship between the frequency and position in the sample:

$$\omega = \gamma G z \tag{1}$$

The intrinsic intensity of magnetization can then be estimated in a method described later in this section. The intrinsic intensity of magnetization is proportional to the linear density, $N(z)$:

$$M_0(\omega) = k N(z), \tag{2}$$

where

$$N(z) = \int_{A_{xy}} \rho(x,y,z) dx\, dy \tag{3}$$

To determine the linear density from Eq. 2, the calibration constant k must be determined. The factor k depends on several quantities, such as the receiver gain, the static magnetic field, and the quality factor Q of the receiving coil. Some of these factors, particularly the quality factor, may change during the experiment. Consequently, it is desirable to include a reference standard in the imaged volume. The proportional factor can be determined at any time during the experiment from the following equation obtained by integrating Eq. 2:

$$k = \frac{\int_{\Delta\omega_r} M_0^r(\omega) d\omega}{\int_{\Delta Z_r} N^r(z) dz} \tag{4}$$

The fluid saturation distribution can be determined by the ratio of the linear density to the initial linear density determined with the fully saturated core sample:

$$S(z) = N(z) / N_i(z) \tag{5}$$

It is assumed that material outside the core sample does not contribute to the observed signals. The porosity distribution can be determined by

$$\phi(z) = N_i(z) / \rho_l A_c \tag{6}$$

We consider now the determination of the intrinsic intensity of magnetization from the observed amplitude of the profile images. The observed signal depends on the transverse and

longitudinal relaxation properties of the fluid in the porous media and various experimental parameters, in particular the echo time (TE) and repetition time (TR). If the relaxation processes can be suitably represented by parameters T_1 and T_2, and the parameters are uniform throughout the medium, the relation between the observed and intrinsic intensity of magnetization can be expressed as follows (Mandava et al., 1990):

$$M(\omega,TE,TR) = M_0(\omega) f(T_1,TR) g(T_2,TE) \tag{7}$$

The effects of longitudinal relaxation can be eliminated if sufficiently long repetition time TR is used; the function $f(T_1,TR)$ can be taken to be unity when $TR \geq 5T_1$. This condition was adhered to so the effects of longitudinal relaxation will not be considered further.

In previous work, transverse relaxation was represented with a single exponential model using a single, averaged value for T_2. For this situation, the correction factor is :

$$g(T_2,TE) = \exp(-TE / T_2) \tag{8}$$

This factor can be used in Eq. (7) for the both core region and reference sample. The value of T_2 for the core region was determined during the initial, fully saturated state.

The accuracy of this model will be limited for porous samples with a distribution of characteristic pore sizes. The rate of relaxation can depend on the sizes of the pores, as well as local surface composition. Since these typically vary throughout porous media, the relaxation of saturating fluids in porous media may not be well represented by a single-exponential model. Another consideration is that the distribution of pore sizes occupied by the observed fluid phase will change as saturation changes. Consequently, the observed relaxation may be a function of saturation. Also, relaxation in heterogeneous rocks may be a function of location as well.

We have developed a new approach in which the effects of spatial variation and saturation dependence of transverse relaxation, as well as non-single-exponential relaxation behavior, can be largely taken into account for determining fluid saturations and porosity. The method involves the acquisition of profile images for several different values of TE and the determination of intrinsic intensity of magnetization by extrapolation of echo amplitude to zero echo time ($TE = 0$) in a model of intensity evolution in the frequency domain. Using this approach, better estimates for the intrinsic intensity of magnetization are obtained and transverse relaxation is characterized on a pixel-by-pixel basis.

Several different models will be considered for the representation of the effects of transverse relaxation on the observed intensity. A multi-exponential approach has frequently been used to represent relaxation in porous media (Timur, 1969; Gallegos et al., 1988). In this model,

the porous medium is represented as a set of discrete groups of relatively uniform pore sizes. Allowing for the use of different relaxation parameters at different positions, the observed intensity of magnetization corresponding to the i[th] pixel can be represented by

$$M(\omega_i,TE) = \sum_{j=1}^{N_c} M_{0j}(\omega_i)\exp(-TE / T_{2ij}) \tag{9}$$

Single-exponential relaxation is obtained for the special case of $N_c = 1$.

A relatively compact representation for intensity relaxation is provided by the stretched exponential (Kenyon et al., 1988)

$$M(\omega_i,TE) = M_0(\omega_i)\exp(-TE / T_{2i})^{\alpha_i} \tag{10}$$

The stretched exponential was shown to arise from a distribution of single exponential relaxation times weighted toward short times. They showed that a stretched exponent α of 0.67 results from a Gaussian distribution of relaxation times (Banavar et al., 1989).

Estimates for the relaxation parameters are obtained by nonlinear regression through minimization of the following performance index for the i[th] pixel :

$$J = \sum_{j=1}^{n} [M^{obs}(\omega_i,TE_j) - M^{cal}(\omega_i,TE_j)]^2 \tag{11}$$

where the calculated values M^{cal} are provided by the representations in Eqs. (9) or (10). For the multi-exponential model, estimates would be obtained for $(M_{0j}(\omega_i), T_{2ij})$, $j = 1, ..., N_c$, for each pixel. The intrinsic intensity of magnetization for the i[th] pixel is the sum:

$$M_0(\omega_i) = \sum_{j=1}^{N_c} M_{0j}(\omega_i) \tag{12}$$

For the stretched exponential model, estimates for $M_0(\omega_i)$, T_{2i}, and α_i are obtained for each pixel.

A useful statistical criterion for selection of the appropriate number of terms for the multi-exponential model is the F-test (Beck and Arnold, 1977; Draper and Smith, 1981). One can test whether a more complete model is warranted by comparing a tabulated value with a statistic calculated using values of the residual sum of squares obtained using the more complete model

(with N_c components) with the previous model (with N_c-1 components). The calculated statistic is

$$F = \frac{[RSS(N_c - 1) - RSS(N_c)] / q}{RSS(N_c) / (n - m)} \tag{13}$$

If the tabulated value exceeds the calculated value, one may conclude (at the specified level of significance) that the available data do not warrant inclusion of the additional terms in the more complete model. For nonlinear regression, the confidence level is said to be approximate (Beck and Arnold, 1977).

Various simplified situations may also be of interest. For example, one could consider multi- or stretched-exponential behavior, but assume that the relaxation parameters are uniform. This could be handled with minor modifications to the previous formulation. We will make use of a simplified procedure to determine the average porosity in the Results and Discussion section. In this situation, the integrated signal from either the core or reference region is represented with the multi- or stretched-exponential models.

METHODS

IMAGING PROCEDURES

All NMR measurements were made with a GE 2-Tesla CSI-II imager/ spectrometer with 31 cm magnet bore and equipped with 20 G/cm shielded gradient coil. Since the birdcage coil has a good quality in RF homogeneity over the coil volume, the assumption of homogeneity of quality factor, Q , is justified. A simplified version of the spin-warp (Mansfield and Morris, 1982) pulse sequence, in which slice and phase encoding gradients are eliminated, was used for acquiring longitudinal profile images (Gummerson et al., 1979; Blackband et al., 1986; Assink et al., 1988; Mandava et al., 1990). Multiple echoes with 12-15 different values of TE were used to acquire profiles for each data set. This profile imaging technique provides for rapid acquisition at large S/N (Signal-to-Noise), thus avoiding flow artifacts during the dynamic experiments.

EXPERIMENTAL PROCEDURES

Laboratory measurements of porosity and saturation distributions were conducted on a large number of core samples. Most core samples were prepared in cylindrical shape with the dimension of 2.54 cm in diameter and 7 cm in length. Building limestones A and B were 3.5 and

2 cm in length, respectively. The core samples were mounted inside a Plexiglass cylindrical tube and epoxy resin (Stycast ® 2651) was used for curing the core with the Plexiglass. The values of T_2 and T_2^* in the cured epoxy resin and Plexiglass are much shorter than those for the fluid saturated rocks; therefore, contributions from the core holder to the total signal were insignificant. In the two-phase immiscible displacement experiment, n-octadecene was used as the oil phase and deuterium oxide (D_2O) was used as the aqueous phase. In the experiments in which only the porosity was investigated, the samples were saturated with distilled water. To prepare the epoxy-cured core sample, it was evacuated for four hours under 1 in. Hg at room temperature. Ten pore volumes of the oil phase were introduced to the evacuated core for three days while kept at 1 in. Hg. To ensure that complete saturation was attained, another ten pore volumes of the oil phase were injected through the epoxy-embedded core. A reference sample (Mitchell et al., 1986; Chang et al., 1990) consisting of a gel of agarose powder and 0.005M $CuSO_4$ solution was taped on to the core holder as a reference standard for the calibration of signal intensity.

RESULTS AND DISCUSSIONS

We first demonstrate the importance of considering spatial or saturation dependence of transverse relaxation for determination of saturation distribution. Measurements were performed on a relatively uniform building limestone sample. Flow direction (longitudinal) MRI proton intensity profiles were acquired at various fluid states. At each state several profiles with different echo times ranging from 2.5 ms to 50 ms were taken so that the intrinsic intensity of magnetization and T_2 values could be obtained on a pixel-by-pixel basis. Figure 1 shows three pairs of saturation profiles corresponding to initial saturation and two different states during an imbibition process. The initial state corresponds to complete saturation with n-octadecene. The partial saturation states were obtained after 1.25 and 21 pore volumes of D_2O were injected, respectively. For comparison, two approaches have been used for calculating the saturation profiles. In the first approach, only a single, averaged T_2 value for the core region, measured at complete saturation, is used for determining the intrinsic intensity of magnetizations at all saturation levels (see Eqs. (7) and (8)). That is, effects of spatial variation and saturation dependence of T_2 have been ignored. In the second approach, the intrinsic intensity of magnetization and T_2 are estimated pixel-by-pixel, thus allowing spatial variation and saturation dependence of T_2. Single-exponential behavior was assumed (i.e., N_c =1 in Eq. (9)), and estimates were obtained by linear regression after taking the natural logarithm of both sides of Eq. 9.

Comparing the two profiles corresponding to initial saturation, we found that the spatial variation of T_2 at full saturation seemed negligible in this sample. This is consistent with the fact

that this core sample appeared relatively uniform in mineral constituency and in macroscopic structure. However, it is observed that the saturation profiles calculated at low saturations using the two approaches show sizeable departures due to saturation dependence of T_2. Even without considering any possible multi-exponential relaxation behavior for this core sample, it is clear that the effects of saturation dependence on transverse relaxation must be considered for accurate estimation of saturation. This effect is further demonstrated by the average value of T_2 , which was 13.9 ms at full saturation and decreased to 9 ms after 21 pore volume of D_2O were injected. Our studies with other rocks indicate that saturation dependence of relaxation is a generic property.

Experiments on several fully saturated samples were performed in order to evaluate the utility of different relaxation models for quantitative determination of the porosity. First, the integrated signal from the core and reference regions were analyzed to determine the most appropriate number of components for the multi-exponential model. A sequence of nonlinear regressions were performed using different numbers of components (i.e., values of N_c in Eq. (9)); a Marquardt-Levenberg method (IMSL, 1987) was used to perform the minimizations.

Regression results for an Indiana limestone sample are summarized in Table 1. A substantial reduction in the residual sum of squares was obtained when using a bi-exponential representation as compared to a single exponential. Little further reduction was obtained using a tri-exponential representation. The measured values of intensity of magnetization are plotted with the calculated values determined with the single- and bi-exponential models in Fig. 2. The latter model provides a much more precise fit of the data. The selection of the bi-exponential model is also supported by the F-test (see Table 1). Values of the average porosity were calculated using intrinsic intensity of magnetization estimated with the single-, bi-, and stretched-exponential model and compared to the value determined gravimetrically. The value for the porosity obtained using the bi-exponential model was 17.7%, which is within 5% of the value obtained gravimetrically (which was 16.9%). The differences between values calculated using the single- and stretched-exponential models and the gravimetric values were 25% and 26%, respectively. Further validation of the selection of the bi-exponential model for this case was provided by a thin section analysis that revealed a very heterogeneous structure with pore volume comprised of primary intergranular pores and micropores. Fluid in the larger intergranular pores would likely contribute to the longer relaxation component, while the fluid in the micropores would contribute the shorter component.

Similar analyses were conducted with two different samples of building limestone. For these samples, the bi-exponential was again chosen by the model selection procedure. Average porosity values for these samples calculated using the bi-exponential model were within 1% of the gravimetric values. Differences of 5% and 14% were obtained with the single-exponential model, while the stretched exponential provided very poor estimates of the average porosity (see Table 2).

We next investigated the determination of porosity profiles by carrying out the estimation procedures on a pixel-by-pixel basis. For each sample, the selection of the number of components was examined for a few pixels. In all cases, the bi-exponential was selected by the procedure. Regression results for specific pixels for building limestone A are summarized in Table 3. The bi-exponential model was then used to obtain estimates of the intrinsic intensity of magnetization for each pixel. The porosity profile for the Indiana limestone is shown in Fig. 3. The average values for the porosity profiles for each sample were calculated and are listed in Table 2. The resulting estimate for each case is within 3% of the gravimetric values.

CONCLUSIONS

We have developed procedures whereby porosity and fluid saturation distributions in porous rocks can be determined accurately using NMR imaging measurements. We found that accurate fluid quantitation requires consideration of spatial variation and saturation dependence of transverse relaxation. This can be handled by performing multiecho profile image acquisitions with extrapolation to obtain the intrinsic proton intensity of magnetization. Careful consideration of an appropriate model for representation of transverse relaxation is also important for accurate quantitation. We used a multi-exponential representation of the transverse relaxation with a statistical procedure for selection of the appropriate number of components. The bi-exponential representation was most appropriate for the limestone samples we examined.

Nomenclature

A_c = cross section of sample

A_{xy} = cross section of the experimental volume

f = correction function for T_1 effect

g = correction function for T_2 effect

G = magnitude of the applied field gradient

J = performance index

k = calibration constant

m = number of components in more complete model

M = intensity of magnetization in the rotating frame

M^{cal} = calculated intensity of magnetization

M^{obs} = observed intensity of magnetization

M_0 = intrinsic intensity of magnetization

M_0^r = intrinsic intensity of magnetization corresponding to reference standard

n = number of data

N = linear proton density

N_c = number of components

N_i = linear density corresponding to fully saturated core

N^r = linear density corresponding to reference standard

q = difference between number of components in simpler and more complete model

RSS = residual sum of squares

$RSS(N_c)$ = residual sum of squares using model with N_c components

S = fluid saturation

TE = echo time

TR = repetition time

T_1 = longitudinal relaxation time

T_2 = transverse relaxation time

x, y, z = cartesian coordinates

Greek letters

α_i = a strecthed exponent corresponding to i th pixel

γ = proton gyromagnetic ratio

ρ = proton density in experimental volume

ρ_l = proton density in observed fluid phase

ϕ = porosity

ω = angular frequency

$\Delta\omega_r$ = angular frequency across reference standard

Δz_r = length across reference standard

ACKNOWLEDGMENT

The authors gratefully acknowledge partial support of this work by the Department of Energy (Grant # DE-FG07-89BC14446), the Ind-Univ. Cooperative Program, and the Center for Energy and Mineral Resources of Texas A&M University.

REFERENCES

Assink, R. A., Caprihan, A., and Fukushima, E., 1988, Density Profiles of a Drainage Foam by Nuclear Magnetic Resonance Imaging, *AIChE J.*, v.34, p.2077-79

Baldwin, B. A., and Yamanashi, W. S., 1986, Detecting Fluid Movement and Isolation in Reservoir Cores Using Medical NMR Imaging Techniques, SPE/DOE 14884, p.39-42

Banavar, J. R., and Schwartz, L. M, 1989, Probing Porous Media with Nuclear Magnetic Resonance, in J. Klafter and J. M. Drake, ed., *Molecular Dynamics in Restricted Geometries*, John Wiley & Sons, New York, p.273-309

Beck, J. V. and Arnold, K. J., 1977, *Parameter Estimation in Engineering and Science*, John Wiley & Sons, New York City

Blackband, S., Mansfield P., Barnes, J. R., Clague, A. D. H., and Rice, S. A., 1986, Discrimination of Crude Oil and Water in Sand and in Bore Cores with NMR Imaging, *SPE Formation Evaluation* 1, p. 31-34

Chen, J., Dias, M. M., Patz, S., and Schwartz, L. M., 1988, Magnetic Resonance Imaging of Immiscible Fluid Displacement in Porous Media, *Phys. Rev. Lett.*, v. 61, p.1489-92

Chen, S., Kim, K.-H., Qin, F., and Watson, A. T., 1991, Quantitative Imaging of Multiphase Flow in Porous Media, *Magn. Reson. Imaging*, In Press

Chang, C.-T., Robinson, J. W., Edwards, C. M., Mandava, S., and Watson, A. T., 1990, An Agarose Gel Reference Standard for Use In MRI Determination of Porosity and Fluid Saturations in Porous Media, Research Report 90-01, Engineering Imaging Laboratory, Texas A&M University

Draper, N. R. and Smith, H., 1981, *Applied Regression Analysis*, second edition, John Wiley & Sons, New York City

Edelstein, W. A., Vinegar, H. J., Tutanjian, P. N., and Romer, P. B., and Mueller, O. M., 1988, NMR Imaging for Core Analysis, *SPE* 18272, p. 101-112

Gallegos, D. P. and Smith, D. M., 1988, A NMR Technique for the Analysis of Pore Structure: Determination of Continuous Pore Size Distribution, *J. Colloid Inter. Sci.*, v 122, no. 1, p. 143-153

Gummerson, R. J., Hall, C., Hoff, W. D., Hawkes, R., Holland, G. N., and Moore, W. S., 1979, Unsaturated Water Flow within Porous Materials Observed By NMR Imaging, *Nature*, v. 281, no. 6, p.56-57

Halperin, W. P., D'Orazio, F., Bhattacharja, S., and Tarczon, J. C, 1989, Magnetic Resonance Relaxation Analyses of Porous Media , in J. Klafter and J. M. Drake, ed., *Molecular Dynamics in Restricted Geometries*, John Wiley & Sons, New York, p.311-350

International Mathematical and Statistical Libraries, Inc., 1987, *Math/Library User's Manual; Fortran Subroutines for Mathematical Applications*, IMSL, Houston

Kenyon, W. E., Day, P. I., Straley, C., and Willemsen, J. F., 1988, A Three-Part Study of NMR Longitudinal Relaxation Properties of Water-Saturated Sandstones, *SPE formation Evaluation* 3, p. 622

Mandava, S. S., Watson, A. T., and Edwards, C. M., 1990, NMR Imaging of Saturation During Immiscible Displacements, *AIChE J.*, v. 36, p. 1680-1686

Mansfield, P. and Morris, P. G., 1982, *NMR Imaging in Biomedicine*, Academic Press, San Francisco

Mitchell, M. D., Kundel, H. L., Axel, L., and Joseph, P. M., 1986, Agarose as a Tissue Equivalent Phantom Material for NMR Imaging, *Magn. Reson. Imaging*, v. 6, p. 287

Richmond, P. C., and Watson, A. T., 1990, Estimation of Multiphase Flow Functions From Displacement Experiments, *SPE Reservoir Engineering*, February, p. 121-127

Timur, A., 1969, Pulsed Nuclear Magnetic Resonance Studies of Porosity, Movable Fluids, and Permeability of Sandstone, *J. Pet. Tech.*, v. 21, p. 775-786

Watson, A. T., Kim, K.-H., Chen, S., and Mejia, G., 1991, Subtask 2 of DOE Annual Report No. DE-FG07-89BC14446

Table 1. Regression Results for Indiana Limestone

Components in Model (N_c)	RSS (scaled *)	R^2	F -value +	$F_{.95}(q, n-m)$
1	90.8	0.990		
2	1.29	1.000	450	3.81
3	1	1.000	1.8	3.89

* Scaled to unity for tri-exponential model (N_c=3).

\+ Calculated with present and previous model.

Table 2. Porosity Estimates Using Different Relaxation Models

Samples	Porosity (% -Error)				
	Gravimetric	Integrated Signal			Average Distribution (Bi-Exp.)
		S-Exp.	Bi-Exp.	Stretch-Exp.	
Bldg Limestone A	18.9	21.4(14%)	19.1(%)	26.0(38%)	19.4(3%)
Bldg Limestone B	19.2	21.1(25%)	19.1(%)	29.5(54%)	19.2(0%)
Indiana Limestone	16.9	20.1(5%)	17.7(5%)	21.3(26%)	17.5(3%)

Table 3. Regression Results for Building Limestone A

60th pixel

Components in Model (N_c)	RSS (scaled *)	R^2	F -value +	$F_{.95}(q, n-m)$
1	5.57	0.999		
2	1.03	1.000	33.1	3.68
3	1	1.000	0.2	3.74

75th pixel

Components in Model (N_c)	RSS (scaled *)	R^2	F -value +	$F_{.95}(q, n-m)$
1	4.99	0.997		
2	1.04	0.999	28.4	3.68
3	1	0.999	0.3	3.74

* Scaled to unity for tri-exponential model (N_c=3).

\+ Calculated with present and previous model.

Figure Caption

Fig. 1. Saturation profiles calculated using two different methods

Fig. 2. Measured intensity with values calculated using single- and bi-exponential models (Indiana limestone)

Fig. 3 Porosity profile for Indiana limestone

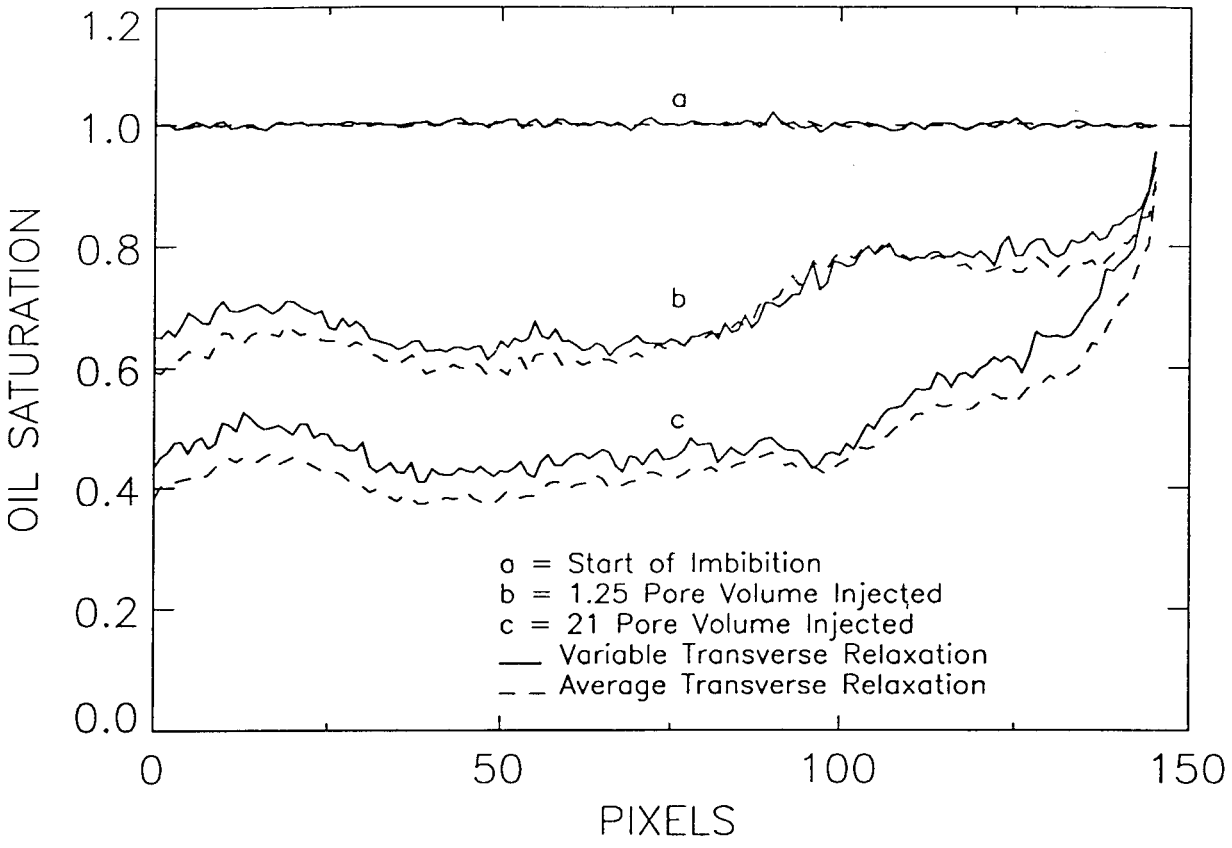

Fig. 1. Saturation profiles calculated using two different methods

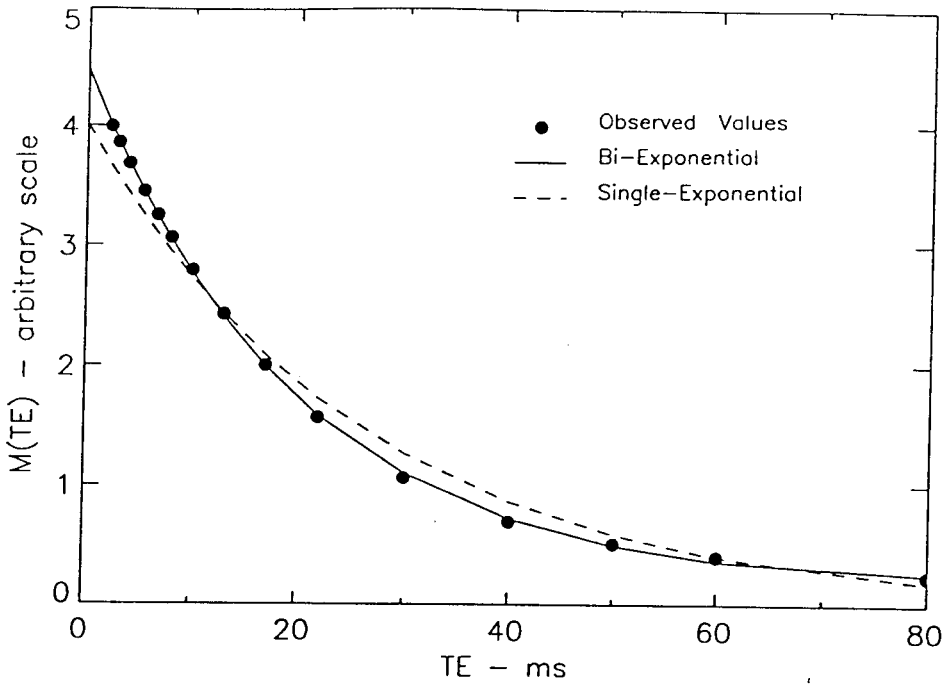

Fig. 2. Measured intensity with values calculated with single- and bi-exponential models (Indiana limestone)

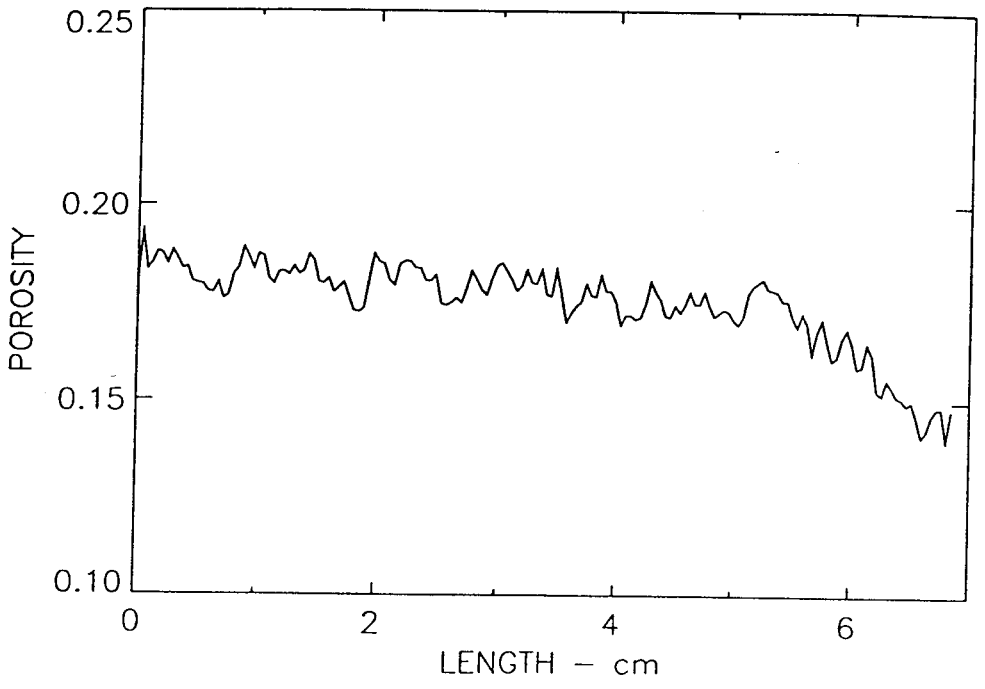

Fig. 3. Porosity profile for Indiana limestone